

CHAPTER 5

Characterisation

Sl. No.	Contents	Page
5.0	Introduction	64
5.1	Chemical analysis	64
5.2	X - ray diffraction analysis	67
5.3	The Laue method	69
5.4	Specific gravity of crystal	71
5.5	Indices of the grown faces	72
5.6	Single crystal rotation	77
	List of Tables	
	Caption to Figures	
	References	

CHARACTERISATION

5.0 Introduction:

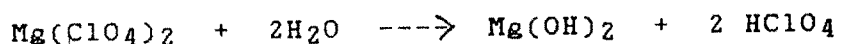
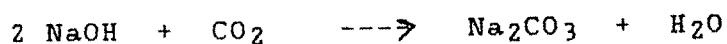
Ammonium-Hydrogen-d-tartrate (d-AHT) crystals grown by gel method (cf. Chapter IV) were characterised by different chemical and physical methods. Quantitative chemical analysis was used to check the chemical constitution and x-ray diffraction technique was used to determine the lattice parameters. The single crystalline character was tested by laue diffraction method.

5.1 Chemical analysis:

Microchemical analysis was carried out to determine elemental content present in d-AHT $\text{NH}_4\text{HC}_4\text{H}_4\text{O}_6$ crystals. A fairly big size d-AHT crystal was selected and cut into two parts, one part was used to determine the carbon and hydrogen content and the other for nitrogen by Duma's method. Carbon, hydrogen, nitrogen and oxygen atoms were found to be present by the following quantitative method.

a) Analysis for Carbon and Hydrogen:

Carbon and hydrogen estimation was carried out by Paigal standard method (Hendrickson et al 1970) using Coleman C-H analyzer. A weighed portion of the compound was burnt in oxygen, over hot copper oxide at about 700 Deg C. Carbon dioxide and water vapour were produced and were individually captured and weighed in absorption tubes. For CO_2 , the reagent used for adsorption was sodium hydroxide coated over soda asbestos, and magnesium perchlorate $\text{Mg}(\text{ClO}_4)_2$ was used for water. The chemical reactions taking place were as under:



In the present case, the amounts of sample taken and those collected of CO₂ and H₂O were as under:

Amount of sample (d-AHT) used = 5.650 mg

Amount of CO₂ collected = 6.074 mg

Amount of H₂O collected = 2.554 mg

From these values, the percentage of C & H in the sample present were found to be -

% C = 29.31

% H = 5.055

b) Analysis for Nitrogen:

Dumas analysis was used to determine the percentage of nitrogen. The sample (d-AHT) was mixed with cupric oxide (CuO) and was heated to dull-red, which resulted in complete oxidation of the organic material.

The resulting gases were passed over a surface of hot copper to reduce nitrogen oxide to nitrogen. The other more active gases (Chlorine, ozone, carbon-dioxide, etc.) were chemically absorbed and the residual volume of nitrogen was measured carefully at definite temperature and pressure. The weight of nitrogen was calculated (by ideal gas law) and was divided by the initial sample weight to give the fraction of nitrogen in the original compound.

The nitrogen content in the sample was found to be as under:

Initial weight of sample (d-AHT) = 5.089 mg
Vol. of nitrogen collected = 0.3659 ml
By calculation - % N observed = 7.957

c) Estimation of Oxygen:

By the stoichiometric principles of general chemistry (Hendrickson, 1970), the sum of percentages of components equals approximately 100 percent. The sum of the percentages of C, H, and N was found to be (29.31 + 5.055 + 7.957) 42.322, which is less than 100. This meant that oxygen was present in the compound.

$$\begin{aligned} \% \text{ Oxygen} &= 100 - 42.322 \\ &= 55.678 \end{aligned}$$

The above percentage value of oxygen also includes the impurities inherently present in the reacting chemicals, namely ammonium bromide and d-tartaric acid. As a matter of fact, this is supported by the calculation of percentage deviation from the calculated to observed value, given in Table.5.1.

d) Calculated percentage:

The chemical formula of d-AHT is $\text{NH}_9\text{C}_4\text{O}_6$ ($\text{NH}_4 \cdot \text{H} \cdot \text{C}_4\text{H}_4\text{O}_6$) having molecular weight 167.12 (Weast et al, 1964), from which percentage weight of each element in it is given in Table.5.1).

The percentage difference in the observed and calculated values of oxygen mentioned in the last column of Table.5.1 namely + 0.24 accounts for the experiment errors and the assay impurities present in the basic chemicals.

TABLE 5.1

PERCENTAGE OF d-AHT ELEMENTS

Element	Calculated percentage	Observed %age	%age deviation
1. C	28.75	29.31	+ 0.56
2. H	5.43	5.06	- 0.37
3. N	8.38	7.96	- 0.42
4. O	57.4	57.68	+ 0.24

5.2 X-ray diffraction analysis:

X-ray diffraction techniques are useful tools for microstructural investigations. These techniques based on monochromatic radiations are generally more important because the "d" spacing can be calculated from the observed diffraction angles. In laue method we can find the crystallinity of single crystal qualitatively by just observing the nature of the spots. However, powder diffractometry is more commonly used. In diffractometers, the diffracted radiation is usually detected by counter tubes which move through angular range of reflections. The intensities are recorded on synchronously advancing strip charts. An important feature of diffractometers is their

ability to focus into a sharp diffraction line the radiation which is Bragg reflected from an extended specimen area. This improves the sensitivity as well as signal to noise ratio.

There are two different designs of diffractometers. The first one is "The Bragg Brentano xray diffractometer". Here the specimen is mounted in the center of the diffractometer and rotated by an angle θ around an axis in the crystal plane. The counter is attached to an arm rotating around the specimen axis by an angle twice as large as those of the specimen rotation. Only (hkl) planes parallel to the crystal plane contribute to the diffraction intensity. The intensity falls off rapidly for higher order reflections.

The second design of diffractometers utilizes the Seeman Bohlin effect, in which the specimen and focussing circle remain stationary, while the detector tube moves along the circumference of the focussing circle itself. Its main advantage is the constant angle of incidence, which can be kept as small as 5° , thus giving higher diffracted intensities than those obtained by Bragg-Brentano diffractometer in the whole angular range and particularly in the back reflection region.

However, the x-ray diffraction technique has several limitations:

- 1) The information obtained is averaged over a macroscopic area irradiated by x-rays;
- 2) The sample depth examined is limited to the x-ray penetration depth;

3) The information is obtained along the direction parallel to the x-ray direction vector.

In the present study the x-ray diffractometer Philips PM 8203 with PW 1390 channel control and PW 1373 goniometer supply has been used for characterization of single crystals of Ammonium-hydrogen-d-tartrate.

Crystal samples were used to take the x-ray powder diffractograms (Fig.5.1). The figure represents plot of intensity of the diffracted beam vs angle, $2i$, where i is the angle between the incident x-ray beam and the reflecting plane. The $2i$ values obtained were compared with that of the literature values (Azaroff and Buerger). It was found that the experimental values were in good agreement with that of the literature ones, revealing that the grown crystals were ammonium-hydrogen-d-tartrate (d-AHT) crystals.

5.3 The laue method:

The Laue method of x-ray diffraction is a powerful technique for determining the orientation of a crystal. Since the crystals are transparent to x-rays, Laue transmission pattern of the crystals could be easily obtained. It was also used for the purpose of confirming the cleavage plane. The x-ray generator (Phillips No. 1009) with copper target, was operated at 35 KV and 20 mA with unfiltered beam of x-rays. Unicam camera was used to take the photographs.

Apart from its extremely simple experimental arrangement, the laue method allows ready recognition of the point group of the crystal. However, this is limited to the eleven Friedel classes (centrosymmetric groups) out of the 32 point groups. In the present case, for taking the Laue pattern, the x-ray beam was directed normal to the cleavage plane of the specimen. Besides the identification, the Laue patterns were also used for qualitative assessment of crystal perfection.

Sharp and well defined Laue spots were obtained in the case of crystals free from inclusions and having low dislocation density (as measured by etchpit count), whereas relatively distorted Laue spots were obtained with deformed crystals.

The single crystalline character was checked by the Laue x-ray pattern. A typical pattern is shown in figure 5.2. Apart from indicating that the sample is necessarily a single crystal, the sharpness of the Laue spots show that the crystal is fairly perfect.

An orthorhombic crystal has the following projection symmetries (Azaroff and Buerger, 1958).

Direction	[100]	[010]	[001]	[0VW]	[UVW]
Symmetry	2mm	2mm	2mm	m	1

This indicates that it has a 2-fold symmetry axis and two reflected planes perpendicular to all pinacoids.

The photograph is taken with x-ray beam normal to the cleavage plane, which implies 2-fold symmetry and two mirror lines.

5.4 Specific Gravity of crystal:

The specific gravity (SG) of d-AHT was determined by the specific gravity of the bottle. Specific gravity is defined as, the weight of the body divided by the weight of an equal volume of water. The crystal is partially soluble in water, whereas it is insoluble in kerosene which was used to determine the S.G of d-AHT crystals. The observations and calculations are as under:

- i) Wt. of empty specific gravity bottle = W1 = 19.504 gm
- ii) Wt. of S.G. bottle + crystals = W2 = 20.430 gm
- iii) Wt. of S.G bottle + crystals + kerosene = W3 = 60.129 gm
- iv) Wt. of S.G. bottle + kerosene = W4 = 59.66 gm at 23 Deg C
- v) Wt. of S.G. bottle + distilled water=W5 = 69.375 gm at 23°C

$$\begin{aligned}\text{Specific gravity of Kerosene } =g &= \frac{W4-W1}{W5-W1} \\ &= \frac{40.156}{49.871} \\ &= 0.805\end{aligned}$$

$$\begin{aligned}\text{S.G of d-AHT crystal} &= \frac{W2-W1}{(W4-W1)-(W3-W2)} \\ &= \frac{0.926}{40.156 - 39.699} \times 0.805 \\ &= 1.631\end{aligned}$$

The experiment was repeated several times and mean value was taken.

5.5 Indices of the grown faces:

The arrangement of habit planes on a crystal, when allowed to grow freely, follows the symmetry of the crystal and the relative size developments follow successively increasing indices of plane. The law of constancy of angles, a fundamental law of crystallography first observed by Steno, extended by Domenico and later confirmed by Rome de Isle (4) (Philips, 1971), served as a very useful tool for crystal identification. For orthorhombic crystal, all three parameters are different and the interaxial angles are each 90° . For ammonium-hydrogen-d-tartrate (d-AHT), the stereogram was prepared and with its help, faces were indexed.

5.5 (a) Stereographic Projection of d-AHT:

Stereographic projection is a versatile geometric construction quite useful for crystallographic analysis of geometric data obtained from study of a crystal. It is also an attractive medium to represent crystallographic correlations of physical properties of a crystal. It is often used for determining crystal orientation, indexing surface markings such as slip lines, twins, deformation bands, cracks, etch pits, patterns made by magnetic powders for solving crystallographic problems involved in precipitation and overgrowths.

It was used to index the habit faces of the grown d-AHT single crystals in the present study.

The stereographic projection is a projection of spherical space on a plane, the angular relations being preserved on the plane. In crystallography, it is the projection of intersections of the normals to real or fictitious planes of a crystal, infinitesimal in size and imagined to be positioned at the centre of the sphere. In principle, there are infinite number of such planes defined for a crystal. However, in practice, only rational planes are useful since primarily only such planes significantly participate in the physical phenomenon observable with a crystal.

If the lattice parameters and interaxial angles for a crystal are known, the stereographic projection of the crystal can be prepared. Due to discreteness of distinct crystal structure, there are relations between the indices of a crystal plane being projected and the position of the corresponding projection. These result into the so-called zone laws relating the plane indices and indices of the zone to which a plane belongs. The mutual angular relations between various crystal planes represented by their indices are decided by the lattice parameters and the interaxial angles. For constructing the stereogram and analysing its data, Wulff-net is a convenient graphical aid (5) (Dana, 1985). The procedure of constructing the stereogram of d-AHT is described here.

The plane of projection selected was (001), the pole of which was plotted at the centre of the circle (Fig.5.3). The other pinacoids are placed at 90° to each other along the circumference of the stereogram i.e. primitive circle.

To plot other poles, the following method was adopted. The angle between two vectors was defined by their dot product.

$$V^*_{h_1 k_1 l_1} \cdot V^*_{h_2 k_2 l_2} = r_1 r_2 \cos(\theta)$$

where θ = angle between the vectors representing $(h_1 k_1 l_1)$ and $(h_2 k_2 l_2)$

$$\begin{aligned} \cos(\theta) &= \frac{1}{V_1 V_2} V^*_{h_1 k_1 l_1} \cdot V^*_{h_2 k_2 l_2} \\ &= \frac{1}{V_1 V_2} (h_1 a^* + k_1 b^* + l_1 c^*) \cdot (h_2 a^* + k_2 b^* + l_2 c^*) \\ &= \frac{1}{V_1 V_2} h_1 h_2 a^{*2} + k_1 k_2 b^{*2} + l_1 l_2 c^{*2} \\ &\quad + (h_1 k_2 + k_1 h_2) a^* b^* \cos(\gamma^*) \\ &\quad + (k_1 l_2 + l_1 k_2) b^* c^* \cos(\alpha^*) \\ &\quad + (l_1 h_2 + h_1 l_2) c^* a^* \cos(\beta^*) \end{aligned}$$

$$\cos(\theta) = d_1 d_2 [h_1 h_2 / a^2 + k_1 k_2 / a^2 + l_1 l_2 / a^2]$$

Using equation (5.3) the angles between $(111) \wedge (100)$ and $(111) \wedge (001)$ were calculated and (111) was plotted at the calculated angles subtended by (111) with (100) and with (001) .

The angles between different faces were computed on the basis of reported parameters. With the help of the Wulff-net, the two zones defined by (111) with (100) and (111) with (001) were traced out, the pole (111) was plotted where these two zones intersected. In the same way, (121) and (211) poles were also plotted.

For the plotted poles on a zone, zone law (5) was used (Dana, 1985). The zones defined by the pairs (100) and (001) , (010) and (001) and (100) and (010) were drawn first. The first two were perpendicular diameters drawn from plotted pinacoids. The third

was the primitive circle. For e.g., indices of the pole occurring between (uvw) and (x,y,z) and on the zone defined by them will be $(u + x, v + y, w + z)$.

In the same way, the zone defined by (111) and (001) was drawn to intersect the primitive, the intersection being indexed as (110) on both sides. Similarly, the zones defined by the pairs (010) and (111) , (100) and (111) , (010) and (121) , (001) and (121) , (001) and (211) etc were drawn for further necessary poles. Thus with the help of zone law all intersections were indexed. Here on one side, indices are shown without bar, to show the index on opposite side of the axis. Fig.5.3 shows the stereogram of the d-AHT crystal.

5.5 (b) Miller indices for natural habit faces of d- AHT crystal:

Interfacial angles were measured by the optical goniometer. The d-AHT crystal is having one zone parallel to $[001]$. The orthorhombic disphenoidal crystal was used to find out the zone angles. The crystal was stuck with plasticine on the goniometer head such that the edge formed by the two faces was parallel to the goniometer axis. The observations were made by keeping the goniometer under table microscope and focussing all the faces of the zone, one by one. Similarly the angles between the sphenoidal faces were also measured.

Different zones and measured angles were checked for the corresponding match on the stereogram. In the present case, the primitive of the stereogram (Fig.5.3) showing zone (010) and

(100) was the major zone of the crystal. The faces were indexed according to the matched poles. Figs. 5.4 & 5.5 show schematic diagrams of crystals having different habits with symbols of faces. Other habits were indexed by similar comparison.

The planes shown in Fig.5.4 were indexed as follows:

Reference Plane	Designation Index	Reference Plane	Designation Index
1	(110)	I	(1 1 1)
2	(130)	II	($\bar{1}$ $\bar{1}$ $\bar{1}$)
3	($\bar{1}$ 10)	III	($\bar{1}$ 1 $\bar{1}$)
4	($\bar{1}$ 00)	IV	(1 $\bar{1}$ $\bar{1}$)
5	($\bar{1}\bar{1}$ 0)	V	($\bar{2}$ 1 3)
6	($\bar{1}\bar{3}$ 0)	VI	(2 $\bar{1}$ $\bar{2}$)
7	($\bar{1}\bar{1}$ 0)	VII	($\bar{2}$ $\bar{1}$ 3)
8	(100)	VIII	(2 1 $\bar{2}$)

The indices for the reference faces given in Fig.5.5 were as follows:

Reference plane	Designation index
I	($\bar{1}$ $\bar{1}$ 1)
II	(1 1 1)
III	(1 $\bar{1}$ $\bar{1}$)
IV	($\bar{1}$ 1 $\bar{1}$)

From the observations of different crystal habits, it was found that for sphenoidal faces $z(111)$ were always present in the

crystal habit, which were freely grown (except in needle shaped crystals). In orthorhombic disphenoidal and needle shaped crystals additionally four prismatic $m(110)$ faces were always present. In zonal planes, (130) plane was always thinner than other planes implying that growth rate is more in the direction normal to it. (100) plane was broader than other planes.

5.6 Single crystal rotation:

The oscillation photograph is regarded as the fundamental type of single crystal photograph. In this method, the crystal is rotated about an axis perpendicular to the incident x-ray beam. This allows many lattice planes to come into the appropriate positions for reflecting the characteristic radiation, due to which spots are produced on the x-ray film. The reflections all appear along straight lines called layer lines, on the cylindrical film. From the values of the layer lines on the photographs with each of the three crystallographic axes as oscillation axis, in turn, we can determine from the heights of the layer lines (6),(7) Fig.5.6, the dimensions a,b and c of the unit cell of the Bravais lattice of the d-AHT crystal.

The lattice parameter, $c = 7.709 \text{ \AA}$ was obtained from the above calculation which was in good agreement with the reported values.

Table-5.2

X ray diffractogram data

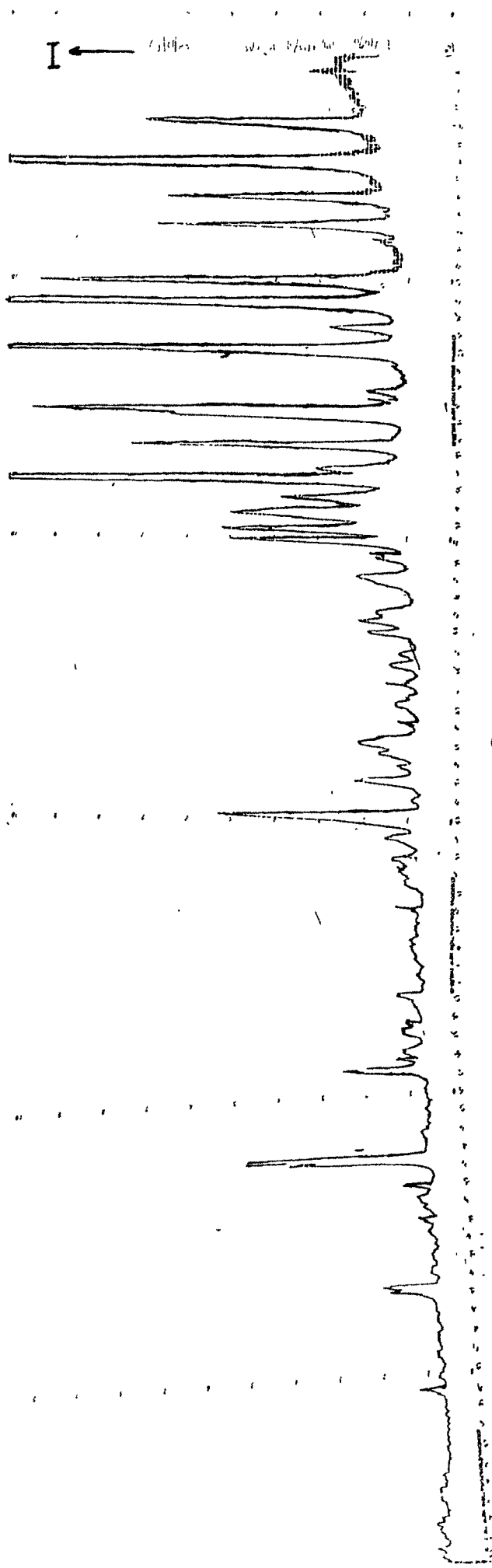
a	b	c	=	11.066	7.843	7.648	
n	2i obs	2i calc		h	k	l	d obs
1	13.80	13.84		1	1	0	6.417
2	16.00	16.02		2	0	0	5.539
3	18.00	18.08		1	1	1	4.928
4	19.70	19.63		2	1	0	4.506
5	24.20	24.13		3	0	0	3.678
6	25.60	25.53		0	2	1	3.480
7	26.80	26.71		3	1	0	3.326
7	26.80	26.83		3	0	1	3.326
7	26.80	26.79		1	2	1	3.326
8	29.20	29.19		3	1	1	3.058
9	30.20	30.28		2	2	1	2.959
10	30.60	30.62		2	1	2	2.921
11	32.40	32.36		4	0	0	2.763
12	33.80	33.76		3	0	2	2.652
12	33.80	33.72		1	2	2	2.652
13	34.40	34.37		4	1	0	2.607
13	34.40	34.30		0	3	0	2.607
13	34.40	34.37		4	0	1	2.607
14	35.50	35.41		3	2	1	2.529
15	36.20	36.16		1	0	3	2.481
16	36.40	36.38		4	1	1	2.468
16	36.40	36.31		0	3	1	2.468
17	36.70	36.62		2	2	2	2.449
18	37.30	37.24		1	3	1	2.411
19	37.90	37.99		1	1	3	2.374
20	38.80	38.90		2	0	3	2.321
21	39.90	39.88		4	2	0	2.259
21	39.90	39.92		2	3	1	2.259
22	40.30	40.23		4	0	2	2.238
23	41.90	41.92		4	1	2	2.156
23	41.90	41.86		0	3	2	2.156
24	42.40	42.44		5	1	0	2.132
24	42.40	42.38		3	3	0	2.132
25	43.10	43.13		3	0	3	2.099
25	43.10	43.10		1	2	3	2.099
26	44.20	44.13		5	1	1	2.049
27	44.70	44.73		3	1	3	2.027
28	46.70	46.68		4	2	2	1.945
29	48.40	48.30		1	0	4	1.881
30	48.60	48.64		1	4	1	1.873
30	48.60	48.56		4	0	3	1.873
31	48.80	48.72		5	2	1	1.866
31	48.80	48.89		3	3	2	1.866
32	49.40	49.41		6	0	0	1.845
32	49.40	49.31		2	4	0	1.845
32	49.40	49.42		4	3	1	1.845
33	50.10	50.02		4	1	3	1.821
34	50.80	50.86		6	1	0	1.797
34	50.80	50.82		2	4	1	1.797
35	50.90	50.86		6	1	0	1.794
35	50.90	50.93		6	0	1	1.794
35	50.90	50.82		2	4	1	1.794

Table-5.2
X-ray diffractogram data

a	b	c	=	11.066	7.843	7.648

n	2 θ obs	2 θ calc	h	k	l	d obs

36	52.80	51.92	2	1	4	1.759
37	52.80	52.88	3	4	0	1.734
37	52.80	52.81	2	3	3	1.734
38	53.80	53.88	4	3	2	1.704
39	54.00	54.02	3	0	4	1.698
39	54.00	53.99	1	2	4	1.698
40	54.20	54.23	4	2	3	1.692
41	55.20	55.30	6	0	2	1.664
41	55.20	55.20	2	4	2	1.664
42	56.40	56.43	6	2	1	1.631
43	56.60	56.63	6	1	2	1.626
44	62.70	62.76	2	5	1	1.482
45	62.90	62.85	6	3	1	1.478
45	62.90	62.98	4	4	2	1.478
46	64.40	64.39	5	0	4	1.447
47	64.70	64.74	7	2	1	1.441
47	64.70	64.67	5	4	1	1.441
47	64.70	64.79	1	5	2	1.441
48	65.70	65.61	5	1	4	1.421
49	66.20	66.13	3	0	5	1.412
49	66.20	66.11	1	2	5	1.412
50	66.60	66.62	2	5	2	1.404
51	66.80	66.71	6	3	2	1.400
52	71.40	71.50	4	1	5	1.321
52	71.40	71.45	0	3	5	1.321
53	73.80	73.85	8	1	2	1.284
53	73.80	73.72	4	5	2	1.284
53	73.80	73.84	3	4	4	1.284
53	73.80	73.78	2	3	5	1.284
54	74.00	74.08	5	5	0	1.281
54	74.00	74.08	1	6	1	1.281
55	74.30	74.38	7	3	2	1.277
56	74.90	74.92	6	4	2	1.268
56	74.90	74.97	4	2	5	1.268
57	75.10	75.03	5	3	4	1.265
57	75.10	75.00	1	0	6	1.265
58	75.70	75.72	3	5	3	1.256
58	75.70	75.63	6	2	4	1.256
59	78.70	78.79	9	1	0	1.216
59	78.70	78.76	7	4	1	1.216
59	78.70	78.65	3	6	1	1.216
59	78.70	78.70	8	0	3	1.216
60	78.90	78.84	9	0	1	1.213
60	78.90	78.87	5	5	2	1.213
60	78.90	78.94	0	5	4	1.213
60	78.90	78.98	0	2	6	1.213
61	84.10	84.00	3	5	4	1.151
61	84.10	84.04	3	2	6	1.151
62	92.60	92.58	6	6	0	1.066
62	92.60	92.66	9	2	3	1.066
63	92.80	92.75	10	2	0	1.065
63	92.80	92.89	1	4	6	1.065



← 2θ

FIG. 5.1



Fig. 5.2 (a)

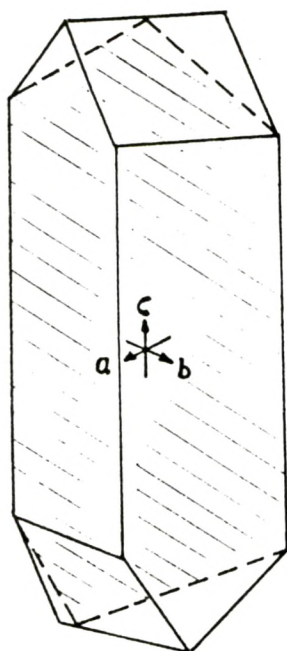


Fig. 5.2 (b) (i)

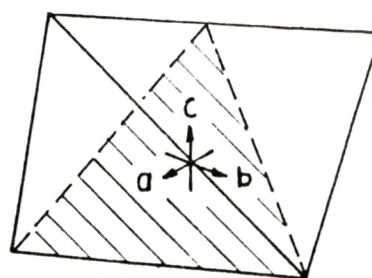


Fig. 5.2 (b) (ii)

Fig. 5.2 (a)

Lane X-ray photograph of single synthetic crystal of d-AHT X-ray beam is normal to cleavage plane (010) of d-AHT.

Fig. 5.2 (b)

Schematic diagram of a cleavage plane shown by shaded region in

- (i) Orthorhombic disphenoidal and
- (ii) Sphenoidal d-AHT crystals

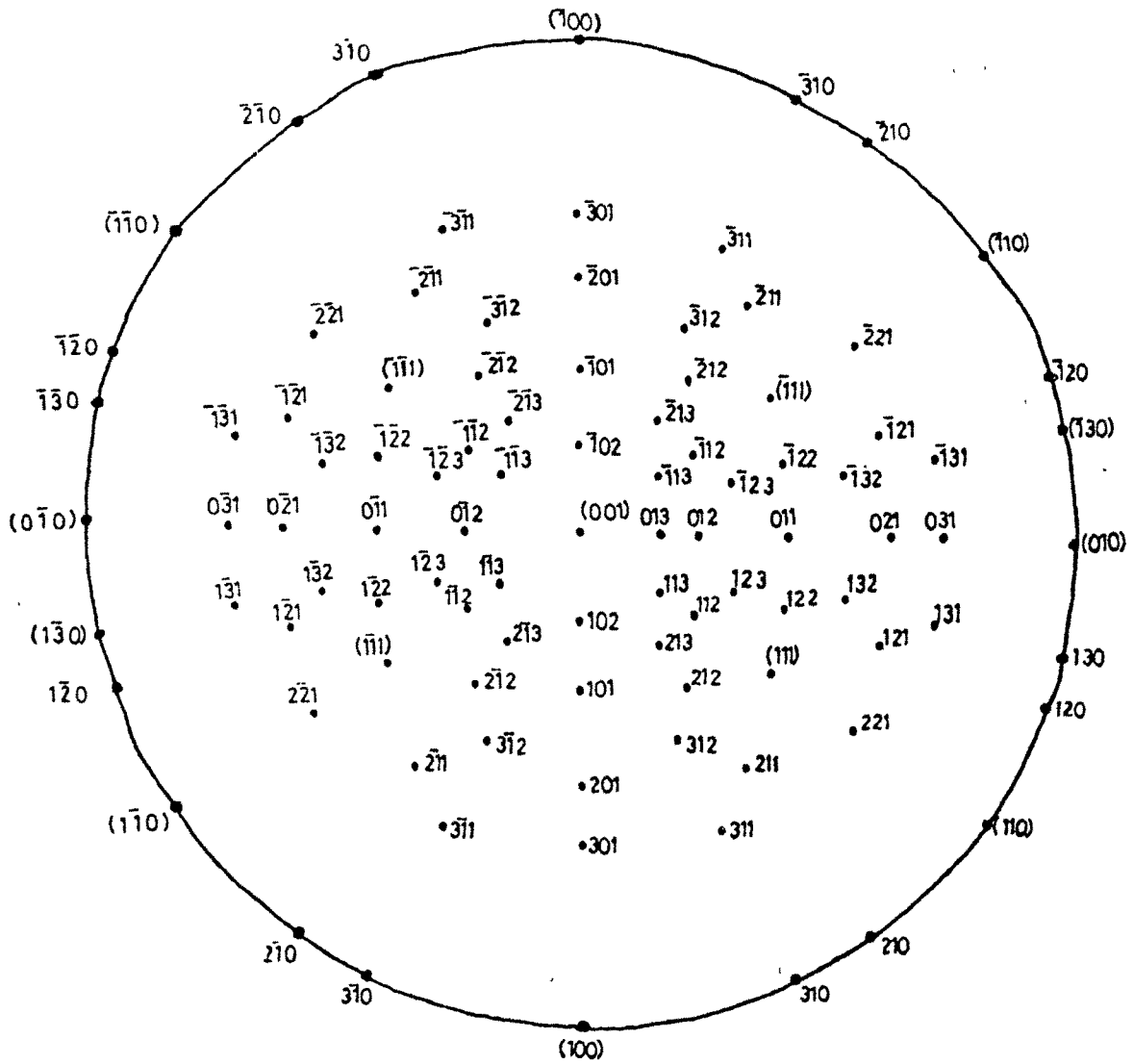


Fig. 5.3

Stereogram of d-AHT crystal

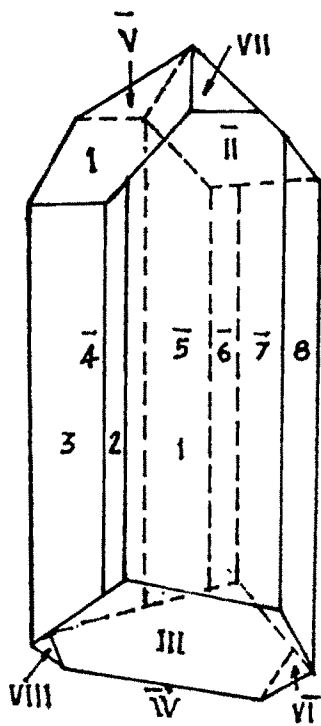


Fig. 5.4 (a)

Sketch of orthorhombic disphenoidal crystal with symbols of faces.

Fig. 5.4 (b)

Observed and calculated interfacial angles.

Reference faces	Observed angle	Calculated angle
1-2	25° 9'	22° 2'
2-3	43° 51' 30"	48° 37'
3-4	55° 30'	54° 40'
4-5	55° 29' 30"	54° 40'
5-6	25° 45' 30"	22° 2'
6-7	43° 14' 30"	48° 37'
7-8	55° 30'	54° 40'
8-1	55° 30'	54° 40'

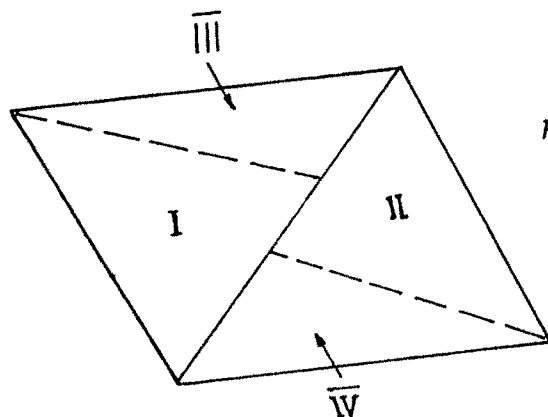


Fig. 5.5 (a)

Sketch of sphenoidal crystal with symbols of faces.

Fig. 5.5 (b)

Observed and calculated interfacial angles

<u>Reference face</u>	<u>Observed angle</u>	<u>Calculated angle</u>
I-II	102°	100° 12'
I-III	101°	102° 31'
I-IV	129°	127° 20'
II-III	127°	127° 20'
II-IV	105°	102° 31'
III-IV	100°	100° 12'



Fig. 5.6 -Single crystal rotation photograph of dAHT. CuK α radiation = 1.5418 Å

LIST OF TABLES

- 5.1 Percentage of d-AHT elements;
- 5.2 Analysis of X-ray powder diffractogram.

CAPTIONS TO FIGURES

- 5.1 X-ray powder diffractogram of d-AHT;
- 5.2 Laue X-ray photograph of synthetic single d-AHT crystal. X-ray beam is normal to cleavage plane (010) of d-AHT.
- 5.3 Stereogram of d-AHT crystal.
- 5.4 Sketch of orthorhombic disphenoidal crystal with symbols of faces.
- 5.5 Sketch of sphenoidal crystal with symbols of faces.
- 5.6 Single crystal rotation photograph of d-AHT
Cu K radiation, $\lambda = 1.5418\text{\AA}$

REFERENCES

01. Hendrickson, J.B; Cram, D.J & Hammond, G.S
Organic Chemistry, 3rd Ed, Mc.Graw Hill,
Kogakusha Ltd, Tokyo, 1970.
02. Weast, R.C; Selby, S.M & Hodgman, C.D
Handbook of Chemistry & Physics, 45th Ed,
The Chemical rubber Co., Ohio, 1964.
03. Azaroff, L.V & Buerger, M.J
The Powder method in x-ray crystallography,
Mc.Graw Hill Book Co.Inc., N.Y, 1958.
04. Phillips, F.C
An Introduction to Crystallography,
ELBS, 1971 edition.
05. Dana, F.S
A Text book of mineralogy,
Asia Publishing House, Bombay, IV Ed, 1985.
06. Henry; N.F.M; Lipson, H & Wooster, W.A
The Interpretation of x-ray diffraction
photographs, MacMillan & Co Ltd, N.Y,
St. Martins Press, 1961, Pg.52.
07. Jeffrey, J.W
Methods in X-ray crystallography,
Academic Press, London & N.Yor., 1971, Pg.31.